Table 1 Backgrounds and characteristics of male and female patients

Factors	Gender		*p* value
	Male	Female	
No. of patients	256 (62.6%)	153 (37.4%)	
Age			
Median (range)	53 (18–73)	59 (23–75)	0.00001
F stage			
F0–2	206 (80.5%)	119 (77.8%)	0.592
F3–4	50 (19.5%)	34 (22.2%)	
Grade (A factor)			
A0–1	163 (63. 7%)	79 (51.6%)	0.026
A2–3	93 (36.3%)	74 (48.4%)	
HCV RNA load 0 week (KIU/mL)			
Median (range)	1500 (100–5000 <)	1280 (100–5000<)	0.384
ALT 0 week (IU/L)			
Median (range)	74.5 (16–504)	59 (19–391)	0.001
BMI			
Median (range)	23.6 (17.5–31.2)	22.1 (16.1–33.9)	0.00033
Alb (g/dL)			
Median (range)	4.0 (3.0–5.2)	3.8 (3.0–4.8)	0.011
LDL-C (mg/dL)			
Median (range)	97 (30–185)	90 (34–174)	0.612
T-Chol (mg/dL)			
Median (range)	167 (85–273)	176 (114–261)	0.0016
PLT count ($\times 10^4$/mm^3)			
Median (range)	17.0 (8.0–31.9)	16.4 (8.1–39.9)	0.350
Amino acid mutation of ISDR			
0–1	200 (78.1%)	121 (79.1%)	0.608
2≤	56 (21.9%)	32 (20.9%)	
Amino acid substitution of core 70			
Wild	177 (69.1%)	114 (74.5%)	0.261
Mutant	79 (30.9%)	39 (25.5%)	
Amino acid substitution of core 91			
Wild	153 (59.8%)	98 (64.1%)	0.403
Mutant	103 (40.2%)	55 (35.9%)	
PEG-IFN adherence			
<80%	41 (17.7%)	42 (30.4%)	0.0066
80%≤	190 (82.3%)	96 (69.6%)	
Ribavirin adherence			
<80%	54 (23.6%)	73 (52.1%)	<0.00001
80%≤	175 (76.4%)	67 (47.9%)	
Age: <60 years			
PEG adherence			
<80%	30 (17.8%)	23 (31.5%)	0.027
80%≤	139 (82.2%)	50 (68.5%)	
Ribavirin adherence			
<80%	27 (16.2%)	31 (42.5%)	0.000029
80%≤	140 (83.8%)	42 (57.5%)	
Age: 60 years≤			
PEG adherence			
<80%	11 (17.7%)	19 (29.2%)	0.147
80%≤	51 (82.3%)	46 (70.8%)	
Ribavirin adherence			
<80%	27 (43.5%)	42 (62.7%)	0.035
80%≤	35 (56.5%)	25 (37.3%)	

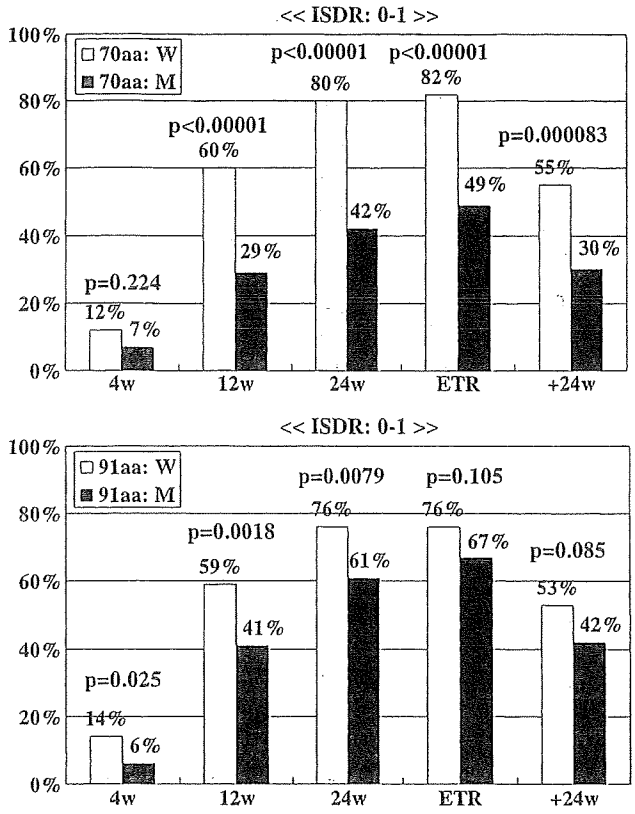

Fig. 1 Relationship between time course of serum HCV RNA negativity and amino acid substitutions in the ISDR and core amino acids 70 and 91. For cases with no or only one amino acid (aa) change in the ISDR, the rates of cEVR, LVR, ETR and SVR were significantly higher in patients with wild type core aa 70 but only the rates of RVR, cEVR, and LVR were significantly higher in patients with wild type core aa 91

Amino acid substitutions

There were no significant differences in the frequency of aa substitutions in the ISDR between males and females. Core aa substitutions at positions 70 and 91 were as follows; 291 (71.1%) were wild type and 118 (28.9%) were mutant at core aa 70, and 251 (61.4%) were wild type and 158 (38.6%) were mutant at core aa 91. There were no significant differences between males and females and between patients below and above 60 years of age.

Virological responses and aa substitutions

The rate of RVR did not differ significantly between males and females. However, more male patients showed HCV RNA negativity at 12 weeks (males vs. females; 60.7 vs. 48.4%, $p = 0.018$), 24 weeks (76.8 vs. 64.2%, $p = 0.0078$) and 48 weeks (78.2 vs. 68.6%, $p = 0.049$), and the proportion of male patients in SVR was significantly higher than that of females (61.3 vs. 37.3%, $p < 0.00001$).

RVR, cEVR and SVR rates were significantly higher in patients with two or more aa mutations in the ISDR compared to patients having no or one aa substitution in that region (20 vs. 11%, $p = 0.044$; 71 vs. 52%, $p = 0.0021$; 66 vs. 49%, $p = 0.0054$, respectively). AA substitution at core position 70 resulted in significantly lower rate of cEVR, LVR, ETR, and SVR (40 vs. 63%, $p = 0.000037$; 51 vs. 81%, $p < 0.00001$; 56 vs. 83%, 41 vs. 57%; $p < 0.00001$, $p = 0.0031$, respectively). Although the patients with the wild type aa at core 91 showed significantly higher rates of RVR and cEVR, the rate of SVR was not significantly higher in those patients ($p = 0.054$).

SVR rates were 30% for patients with no or one aa substitution in the ISDR and the core aa 70 substitution, and were significantly lower compared to those with the wild type aa core 70 (Fig. 1). These findings were not confirmed in patients with no or one aa substitution in the ISDR and the core aa 91 substitution (Fig. 1).

Factors affecting SVR by univariate analysis

Univariate analysis identified nine parameters that influenced non-SVR significantly: female gender, older age, advanced staged liver fibrosis, high viral load, low serum Alb level, low PLT count, no or one aa substitution in the ISDR, aa substitution at core aa 70, and low adherence to RBV (Table 2). The frequency of steatosis and HOMA-IR were significantly ($p = 0.0057$, $p < 0.00001$, respectively) lower in patients with SVR compared with non-SVR (data not shown). However, these factors were not entered in the multivariate analysis because of the absence of the data in many cases.

Factors affecting RVR, cEVR, and SVR by multivariate logistic regression analysis

Multivariate analysis identified four parameters that influenced RVR independently: low HCV RNA load, low serum ALT level, two or more aa mutations in the ISDR and the wild type aa at core position 91 (Table 3).

Concerning cEVR, male gender, mild fibrosis stage, low HCV RNA load, two or more aa mutations in the ISDR, and the wild type aa at core positions 70 and 91 were independent predictors (Table 3).

Concerning SVR, male gender ($p < 0.0001$), low HCV RNA load ($p = 0.013$), high PLT count ($p = 0.0019$), two or more aa mutations in the ISDR ($p = 0.024$), and wild type core aa 70 ($p = 0.0045$) were found to be independent predictors (Table 3).

The predictive values of the combination of gender, PLT count, ISDR and core aa 70 are shown in Fig. 2a. In male patients having PLT of $<15 \times 10^4/mm^3$, and, no or one aa substitution in the ISDR, the SVR rate was 68% when core 70

Table 2 Univariate analysis to identify the factors of SVR

Factors	Negative of HCV RNA after 24 weeks		*p* value
	(−)	(+)	
No. of patients	214 (52.3%)	195	
Gender			
Male	157 (61.3%)	99	<0.00001
Female	57 (37.3%)	96	
Age			
Median (range)	52.5 (18–75)	58 (20–74)	<0.00001
<60 years	155 (58.1%)	112	0.0018
60 years≤	59 (41.5%)	83	
Age: <60 years			
Male	118 (63.4%)	68	0.010
Female	37 (45.7%)	44	
Age: 60 years≤			
Male	39 (55.7%)	31	0.0011
Female	20 (27.8%)	52	
F stage			
F0–2	190 (58.5%)	135	0.000013
F3–4	25 (29.8%)	59	
Grade (A factor)			
A0–1	138 (56.8%)	104	0.130
A2–3	81 (48.5%)	86	
HCV RNA load 0 week (KIU/mL)			
Median (range)	1300 (100–5000<)	1700 (130–5000<)	0.016
ALT 0 week (IU/L)			
Median (range)	66 (16–391)	67 (19–504)	0.892
BMI			
Median (range)	23.0 (17.3–32.4)	23.25 (16.1–33.9)	0.714
Alb (g/dL)			
Median (range)	4.0 (3.2–5.2)	3.8 (3.0–4.8)	0.0088
LDL-C (mg/dL)			
Median (range)	94.5 (31–185)	97.5 (30–182)	0.611
T-Chol (mg/dL)			
Median (range)	169.5 (85–257)	170 (103–273)	0.511
PLT count ($\times 10^4$/mm^3)			
Median (range)	18.2 (8.7–39.9)	15.1 (8.0–31.9)	<0.00001
<15	54 (36.5%)	94	<0.00001
15≤	160 (61.3%)	101	
Amino acid mutation of ISDR			
0–1	156 (48.6%)	165	0.0054
2≤	58 (65.9%)	30	
Amino acid substitution of core 70			
Wild	166 (57.0%)	125	0.0031
Mutant	48 (40.7%)	70	
Amino acid substitution of core 91			
Wild	141 (56.2%)	110	0.054
Mutant	73 (46.2%)	85	
PEG-IFN adherence			
<80%	35 (42.2%)	48	0.063
80%≤	154 (53.8%)	132	
Ribavirin adherence			
<80%	55 (43.3%)	72	0.048
80%≤	132 (54.5%)	110	

Table 3 Multivariate logistic regression analysis to identify independent predictive factors of RVR, cEVR, and SVR

	Odds ratio	95% CI	*p* value
RVR factors selected by stepwise method			
F stage			
F0–2/F3–4	2.924	0.988–8.696	0.053
HCV RNA load 0 week (KIU/mL)			
<1000/1000≤	2.151	1.130–4.082	0.020
ALT 0 week (IU/L)			
<60/60≤	2.165	1.127–4.149	0.020
Amino acid mutation of ISDR			
2≤/0–1	2.371	1.187–4.735	0.014
Amino acid substitution of core 91			
W/M	2.137	1.021–4.464	0.044
cEVR factors selected by stepwise method			
Gender			
Male/female	1.912	1.209–3.021	0.0055
F stage			
F0–2/F3–4	2.079	1.133–3.817	0.018
HCV RNA load 0 week (KIU/mL)			
<1000/1000≤	1.608	1.002–2.577	0.049
PLT count ($\times 10^4$/mm^3)			
15≤/<15	1.427	0.882–2.309	0.148
Amino acid mutation of ISDR			
2≤/0–1	2.512	1.407–4.485	0.0018
Amino acid substitution of core 70			
W/M	2.513	1.508–4.184	0.0004
Amino acid substitution of core 91			
W/M	1.965	1.241–3.115	0.004
SVR factors selected by stepwise method			
Gender			
Male/female	3.704	2.132–6.410	<0.0001
F stage			
F0–2/F3–4	1.812	0.888–3.690	0.103
HCV RNA load0 week (KIU/mL)			
<1000/1000≤	2.024	1.163–3.534	0.013
PLT count ($\times 10^4$/mm^3)			
15≤/<15	2.469	1.394–4.372	0.0019
Amino acid mutation of ISDR			
2≤/0–1	2.148	1.107–4.170	0.024
Amino acid substitution of core 70			
W/M	2.415	1.316–4.444	0.0045
Amino acid substitution of core 91			
W/M	1.433	0.828–2.481	0.199
PEG adherence (%)			
80≤/<80	1.562	0.834–2.926	0.164

W Wild, *M* Mutant

was a wild type but only 16% in patients with mutant at core 70. In female patients, no or one aa substitution in ISDR and $<15 \times 10^4$/mm^3 of PLT count, the SVR rates were as low as 10 or 8%, irrespective of aa substitution at core 70. SVR was only 24% in patients with substitution of core aa 70 even when the PLT count was $\geq 15 \times 10^4$/mm^3. In this study, the combination analysis of PLT count, ISDR, and core aa substitution was useful for predicting non-SVR.

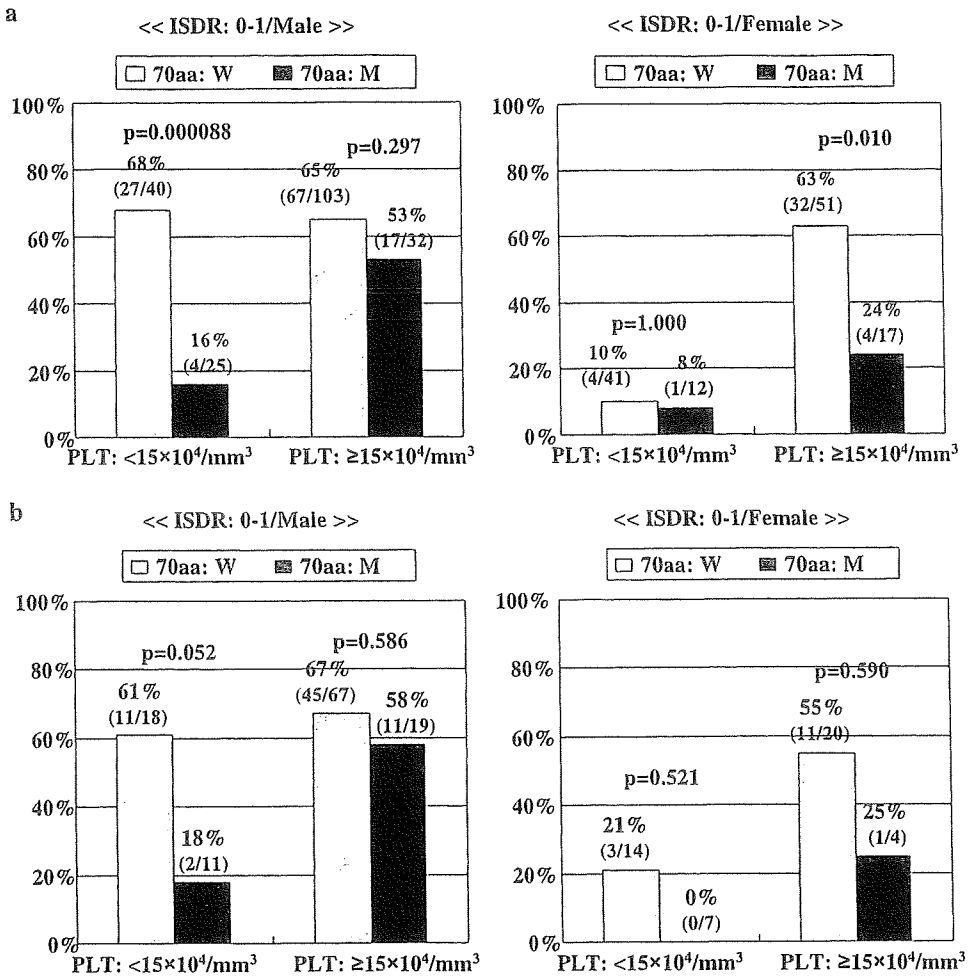

Fig. 2 Relationship between SVR rate and amino acid substitutions in the ISDR and core amino acids 70 and 91, PLT counts and gender difference. The two figures of **a** show the results of *Study 1* and the two figures of **b** show the results of *Study 2*. In male patients with no or only one amino acid (aa) substitution in the ISDR and PLT count of less than $15 \times 10^4/mm^3$, the SVR rate was 68% in those with wild type core aa 70, but only 16% in patients with mutant type of core aa 70, which is significantly different ($p = 0.000088$). There were no significant differences between wild type and mutant type of core aa 70 in the patients with no or one aa substitution in the ISDR and PLT count of over $15 \times 10^4/mm^3$. By contrast, in female patients with no or one aa substitution in the ISDR, there were no significant differences between wild type and mutant type of core aa 70 with PLT count of less than $15 \times 10^4/mm^3$, but there were significant differences between wild type and mutant type of core aa 70 with PLT counts of less than $15 \times 10^4/mm^3$ (**a**). For the patients maintaining over 80% adherences to both PEG-IFN and RBV, in males having no or one aa substitution in the ISDR and PLT counts of less than $15 \times 10^4/mm^3$, a wild type of core aa 70 could predict SVR with a positive predictive value (PPV) of 61% and negative predictive value (NPV) of 82% ($p = 0.052$). However, in male patients with PLT counts of over $15 \times 10^4/mm^3$, core aa 70 was not a useful marker for predicting SVR and non-SVR. The number of female patients with no or one aa substitution in ISDR was too small to reach a definite conclusion (**b**)

Study design 2

The basic features of 201 patients achieving 80% adherences to both PEG-IFN and RBV are as follows: the females were significantly ($p = 0.00006$) older than the males. Iron deposition in liver tissue, alcohol abuse, BMI, serum albumin level, serum ferritin level, and PLT count were significantly higher in males than females. Inflammatory activity was significantly ($p = 0.046$) higher in females than males (data not shown).

AA substitutions in the ISDR were as follows; in males 33 (22.3%) had two or more aa substitutions, in females 8 (15.1%) had two or more aa substitutions. The analysis of core aa position 70 and 91 sequences showed no significant differences in aa substitutions of either core aa 70 or 91 between males and females (data not shown).

In patients less than 60 years of age, SVR rate was significantly higher ($p = 0.0042$) in males than females, but no significant difference was noted between males and females over 60 years old. However, the number of patients over 60 years was small (Table 4).

Table 4 Univariate analysis to identify the significantly different factors between SVR and non-SVR (201 patients received over 80% adherences of both PEG-IFN and RBV)

Factors	Negative of HCV RNA after 24 weeks		*p* value
	(−)	(+)	
No. of patients	111 (55.2%)	90	
Gender			
Male	93 (62.8%)	55	0.00037
Female	18 (34.0%)	35	
Age			
Median (range)	51 (18–70)	56 (23–74)	0.00025
<60 years	91 (60.3%)	60	0.014
60 years≤	20 (40.0%)	30	
Age: <60 years			
Male	79 (66.4%)	40	0.0042
Female	12 (37.5%)	20	
Age: 60 years≤			
Male	14 (48.3%)	15	0.243
Female	6 (28.6%)	15	
F stage			
F0–2	103 (60.9%)	67	0.0012
F3–4	8 (25.8%)	23	
Grade (A factor)			
A0–1	80 (59.3%)	55	0.189
A2–3	31 (47.0%)	35	
HCV RNA load 0 week (KIU/mL)			
Median (range)	1300 (110–5000<)	1280 (130–5000<)	0.351
ALT 0 week (IU/L)			
Median (range)	74 (16–268)	67.5 (19–504)	0.752
BMI			
Median (range)	23.1 (17.3–31.0)	23.6 (16.1–33.9)	0.626
Alb (g/dL)			
Median (range)	3.95 (3.3–5.2)	3.9 (3.0–4.8)	0.079
LDL-C (mg/dL)			
Median (range)	96 (31–185)	97.5 (30–182)	0.865
T-Chol (mg/dL)			
Median (range)	170 (85–248)	170 (105–273)	0.624
PLT count ($\times 10^4/mm^3$)			
Median (range)	18.9 (8.7–30.9)	15.55 (7.2–28.4)	0.00003
<15	23 (35.9%)	41	0.00024
15≤	88 (64.2%)	49	
Amino acid mutation of ISDR			
0–1	84 (52.5%)	76	0.159
2≤	27 (65.9%)	14	
Amino acid substitution of core 70			
Wild	91 (61.5%)	57	0.0037
Mutant	20 (37.7%)	33	
Amino acid substitution of core 91			
Wild	73 (60.3%)	48	0.083
Mutant	38 (47.5%)	42	

Virological responses and aa substitution

The rates of RVR, cEVR, LVR, ETR and SVR in males and females were 12.5 versus 11.3% ($p = 1.000$), 59.6 versus 43.4% ($p = 0.053$), 74.3 versus 50.0% ($p = 0.0018$), 76.2 versus 66.7% ($p = 0.198$), and 62.8 versus 34.0% ($p = 0.00037$), respectively (data not shown). The backgrounds and characteristics of SVR and non SVR patients are shown in Table 4. There were significant differences in gender (male vs. female; $p = 0.00037$), age (<60 years vs. ≥60 years; $p = 0.014$), F stage (F0-2 vs. F3,4; $p = 0.0012$), PLT count ($<15 \times 10^4/mm^3$ vs. $15 \times 10^4/mm^3 \leq$; $p = 0.00024$), and substitution of core aa 70 (wild type vs. mutant, p = 0.0037) between SVR and non-SVR patients. The distribution of fatty change in liver tissue (≤10% vs. 11–33% vs. 34%≤; $p = 0.046$) and the grade of HOMA-IR (1.7 vs. 3.9, $p = 0.0018$) were significantly different between SVR and non-SVR (data not described in Table 4).

Factors affecting SVR by multivariate logistic regression analysis

Male gender ($p = 0.0006$), mild fibrosis stage ($p = 0.027$), and wild type of core aa 70 ($p = 0.043$) were independent predictors of SVR.

Valuable markers for predictions of sustained virological response to peginterferon and ribavirin therapy

Two or more aa mutations in the ISDR, wild type core aa 70, $\geq 15 \times 10^4/mm^3$ of PLT count, and male gender were selected statistically as independent predictors of SVR. We show here SVR rates of the patients having over 80% adherences to both PEG-IFN and RBV (Fig. 2b). In males having no or one aa substitution in the ISRD and PLT count of $<15 \times 10^4/mm^3$, wild type core aa 70 could predict SVR with a positive predictive value (PPV) of 61% and negative predictive value (NPV) of 82% ($p = 0.052$). In females, the SVR rate was very low in those who had substitution of core aa 70, but there was no significant difference between patients with wild type and substitution of core aa 70. The number of female patients was too small to provide a definite conclusion.

Discussion

The present multivariate logistic regression analysis revealed that male gender, low HCV RNA load, high PLT count, and two or more aa mutations in the ISDR and wild type core aa 70 were independent predictors for SVR. PLT count significantly decreased corresponding to the progression to the stage of liver fibrosis in CHC [9, 30, 31].

It has been considered that the low adherence level to PEG-IFN/RBV is a major cause of a significantly lower SVR rate in females and older patients [32]. The percentage of patients having over 80% adherences to both PEG-IFN and RBV was significantly lower in females than males, however, differences in the adherence to PEG-IFN/RBV between males and females were not independent predictive factors of non-SVR.

A recent report from Japan showed six or more mutations in the variable region 3 (V3) of nonstructural protein 5A (NS5A) plus upstream flanking region NS5A (aa 2334–2379), referred to as the IFN/RBV resistance determining region (IRRDR), was a useful marker for predicting SVR, but the ISDR sequence was not valuable for predicting SVR [33]. However, the number of subjects in that study was too small ($n = 45$) to reach an acceptable conclusion.

To elucidate the factors affecting low SVR rate in older female patients, we performed a multivariate logistic regression analysis using patients who achieved ≥80% adherence to both PEG-IFN and RBV. Male gender, stage of mild liver fibrosis, and wild type core aa 70 were independent predictors of SVR. In this study, blood concentration of RBV was determined in fewer than 50% of cases during treatment. Thus we cannot exclude the possibility of the effect of the blood concentration of RBV during treatment on the low SVR rate in females and older patients.

From the present analysis, it was clear that ALT, BMI, Alb, T. Chol, and adherence to RBV differed significantly between males and females, however, these factors were not independent predictors of SVR. There is a report that steatosis is an important cofactor that reduces the SVR rate in genotype 1 infected patients [34], however, such an effect was not seen in this study. Thus we could not identify the factors associated with a significantly lower SVR rate in females than males.

In the present multivariate logistic regression analyses, patients having wild type core aa 91 had significantly higher rates of RVR and cEVR, but not SVR, and patients with wild type core aa 70 had significantly higher rates of cEVR and SVR, but not RVR. Patients having two or more aa substitutions in the ISDR had significantly higher rates of RVR, cEVR, and SVR. Although several possibilities have been considered concerning the effects of aa substitutions of core protein on SVR in PEG-IFN/RBV therapy for CHC patients, the exact mechanisms have not yet been elucidated.

Recent reports have indicated that low serum IP-10 (interferon-γ inducible protein 10 kDa) [35], a higher HCV-specific CD8 cell proliferation potential [36], and a high ratio of Th1/Th2 [37] are good predictors of SVR to

PEG-IFN/RBV therapy. These results indicate the importance of immunological status and immunological response to treatment in patients difficult to treat with PEG-IFN/RBV therapy for CHC.

The present univariate analyses revealed that there were many factors relating to RVR, cEVR, and SVR including LDL-C, HOMA-IR, fatty change in liver tissue, and hyaluronic acid, however some of these factors had not been examined in some participating institutes. We consider that we must perform a prospective mass study using many factors including immunological aspects, viral factors, disease status, and therapeutic aspects to elucidate the reason that older female patients are resistant to a combination of PEG-IFN and RBV therapy in CHC with a high viral load genotype 1b.

In conclusion, our results demonstrated that wild type core aa 70, two or more aa mutations in the ISDR, low viral load, high PLT counts, and male gender are useful markers for predicting SVR.

Acknowledgments We express our thanks to other members of the Study Group of Optimal Treatment of Viral Hepatitis; Hideyuki Nomura, Shin-Kokura Hospital; Yoshiyuki Ueno, University of Tohoku; Hisataka Moriwaki, Gifu University; Makoto Oketani, Kagoshima University Graduate School of Medical and Dental Sciences; Masataka Seike, Oita University; Hiroshi Yotsuyanagi, The University of Tokyo. This study was supported in part by a Grant-in-Aid from the Ministry of Health, Labor and Welfare, Japan.

References

1. Manns MP, McHutchinson JG, Gordon SC, Rustgi VK, Shiffman M, Reindollar R, et al. Peginterferon alfa-2b plus ribavirin for initial treatment of chronic hepatitis C: a randomized trial. Lancet. 2001;358:958–65.
2. Fried MW, Shiffman ML, Reddy KR, Smith C, Marinos G, Gonzales FL, et al. Peginterferon alfa-2a plus ribavirin for chronic hepatitis C virus infection. N Engl J Med. 2002;347:975–82.
3. Hadziyannis S, Sette H Jr, Morgan TR, Balan V, Diago M, Marcellin P, et al. Peginterferon-alfa-2a plus ribavirin combination therapy in chronic hepatitis C. a randomized study of treatment duration and ribavirin dose. Ann Intern Med. 2004;40:346–55.
4. Hiramatsu N, Kurashige N, Oze T, Takehara T, Tamura S, Kasahara A, et al. Early decline of hemoglobin can predict progression of hemolytic anemia during pegylated interferon and ribavirin combination therapy in patients with chronic hepatitis C. Hepatol Res. 2008;38:52–9.
5. Honda T, Katano Y, Urano F, Murayama M, Hayashi K, Ishigami M, et al. Efficacy of ribavirin plus interferon-α in patients aged 60 years with chronic hepatitis C. J Gastroenterol Hepatol. 2007;22:989–95.
6. Sezaki H, Suzuki F, Kawamura Y, Yatsuji H, Hosaka T, Akuta N, et al. Poor response to pegylated interferon and ribavirin in older women infected with hepatitis C virus of genotype 1b in high viral load. Dig Dis Sci 2009;54:1317–24
7. Puoti C, Castellacci R, Montagness F, Zaltron S, Stornaiuolo G, Bergami N, et al. Histological and virological features and follow-up of HCV carriers with normal aminotransferase levels: the Italian Study of the Asymptomatic C Carriers (ISACC). J Hepatol. 2002;37:117–23.
8. Hui CK, Belaye T, Montegrande K, Wright TL. A comparison in the progression of liver fibrosis in chronic hepatitis C between persistently normal and elevated transaminase. J Hepatol. 2003;38:511–7.
9. Okanoue T, Makiyama A, Nakayama M, Sumida Y, Mitsuyoshi H, Nakajima T, et al. A follow-up study to determine the value of liver biopsy and need for antiviral therapy for hepatitis C virus carriers with persistently normal serum aminotransferase. J Hepatol. 2005;43:599–605.
10. Bressler BL, Guindi M, Tomlinson G, Heathcote J. High body mass index in an independent risk factor for non response to antiviral treatment in chronic hepatitis C. Hepatology. 2003;38:639–44.
11. Walsh MJ, Jonsson JR, Richardson MM, Lipka GM, Purdi DM, Clouston AD, et al. Non-response to antiviral therapy is associated with obesity and increased hepatic expression of suppressor of cytokine signaling 3 in patients with chronic hepatitis C, viral genotype 1. Gut. 2006;55:604–9.
12. Patton HM, Patel K, Behling C, Bylund C, Blatt LM, Vallee M, et al. The impact of steatosis on disease progression and early and sustained treatment response in chronic hepatitis C patients. J Hepatol. 2004;40:484–90.
13. Asselah T, Rubbia-Brandt L, Marcellin M, Negro F. Steatosis in chronic hepatitis C: why does it really matter? Gut. 2006; 55:123–30.
14. Romero-Gomez M, Del Mar Viloria M, Andrade RJ, Salmeron J, Diago M, Fernandez-Rodriguez CM, et al. Insulin resistance impairs sustained response rate to peginterferon plus ribavirin in chronic hepatitis C patients. Gastroenterology. 2005;128: 636–41.
15. Bruno S, Camma C, Di Marco V, Rumi M, Vinci M, Cammozzi M, et al. Peginterferon alfa-2b plus ribavirin for native patients with genotype 1 chronic hepatitis C: a randomized controlled trial. J Hepatol. 2004;41:474–81.
16. Everson GT, Hoefs JC, Seeff LB, Bonkovsky HL, Naishadham D, Shiffman ML, et al. Impact of disease severity on outcome of antiviral therapy for chronic hepatitis C: lessons from the HALT-C trial. Hepatology. 2006;44:1675–84.
17. McHutchison JG, Manns M, Patel K, Poynard T, Lindsay KL, Trepo C, et al. Adherence to combination therapy enhances sustained response in genotype-1-infected patients with chronic hepatitis C. Gastroenterology. 2002;123:1061–9.
18. Jeffers LJ, Cassidy W, Howell CD, Hu S, Reddy R. Peginterferon alfa-2a (40kd) and ribavirin for black American patients with chronic HCV genotype 1. Hepatology. 2004;39:1702–6.
19. Muir AJ, Bornstein JD, Killenberg PG, Atlantic Coast Hepatitis Treatment Group. Peginterferon alfa 2b and ribavirin for the treatment of chronic hepatitis C in blacks and non-Hispanic whites. N Engl J Med. 2004;350:2265–71.
20. Poynard T, Marcellin P, Lee SS, Niederau C, Minuk GS, Ideo G, et al. Randomized trial of interferon alpha 2b plus ribavirin for 48 weeks or 24 weeks versus interferon alpha 2b plus placebo for 48 weeks for treatment for chronic infection with hepatitis C virus. International Hepatitis Interventional Therapy Group (IHIT). Lancet. 1998;352:1426–32.
21. Enomoto N, Sakuma I, Asahina Y, Kurosaki M, Murakami T, Yamamoto C, et al. Mutations in the nonstructural protein 5 A gene and response to interferon in patients with chronic hepatitis C virus 1b infection. N Engl J Med. 1996;334:77–81.
22. Akuta N, Suzuki F, Sezaki H, Suzuki Y, Hosaka T, Someya T, et al. Association of amino acid substitution pattern in core protein of hepatitis C virus genotype 1b high viral load and non-virological response in interferon-ribavirin combination therapy. Intervirology. 2005;48:372–80.
23. Donlin MJ, Cannon NA, Yao E, Li J, Wahed A, Taylor MW, et al. Pretreatment sequence diversity differences in the

full-length hepatitis C virus open reading frame correlate with early response to therapy. J Virol. 2007;81:8211–24.
24. Davis GL, Wong JB, McHutchison JG, Manns MP, Harvey J, Albrecht J. Early virologic response to treatment with peginterferon alfa-2b plus ribavirin in patients with chronic hepatitis C. Hepatology. 2003;38:645–52.
25. Ferenci P, Fried MW, Shiffman ML, Smith CI, Marinos G, Goncales FL, et al. Predicting sustained virological responses in chronic hepatitis C patients treated with peginterferon alfa-2a ribavirin. J Hepatol. 2005;43:425–33.
26. Moucari R, Ripault M-P, Oules V, Martinot-Peignoux M, Asselah T, Boyer N, et al. High predictive value of early viral kinetics in retreatment with peginterferon and ribavirin of chronic hepatitis C patients non-responders to standard combination therapy. J Hepatol. 2007;46:596–604.
27. Akuta N, Suzuki F, Kawamura Y, Yatsuji H, Sezaki H, Suzuki Y, et al. Predictive factors of early and sustained responses to peginterferon plus ribavirin combination therapy in Japanese patients infected with hepatitis C virus genotype 1a: amino acid substitutions in the core region and low-density lipoprotein cholesterol level. J Hepatol. 2007;46:403–10.
28. Desmet VJ, Gerber M, Hoofnagle JH, Manna M, Scheuer PJ. Classification of chronic hepatitis: grading and staging. Hepatology. 1994;19:1513–20.
29. Kato N, Hijikata M, Ootsuyama Y, Nakagawa M, Ohkoshi S, Sugimura T, et al. Molecular cloning of the human hepatitis C virus genome from Japanese patients with non-A, non-B hepatitis. Proc Natl Acad Sci USA. 1990;87:9524–8.
30. Okanoue T, Itoh Y, Minami M, Sakamoto S, Yasui K, Sakamoto M, et al. Interferon therapy lowers the rate of progression to hepatocellualr carcinoma in chronic hepatitis C but not significantly in an advanced stage: a retrospective study in 1148 patients. J Hepatol. 1999;30:653–9.
31. Okanoue T, Itoh Y, Minami M, Hashimoto H, Yasui K, Yotsuyanagi H, et al. Guidelines for the antiviral therapy of hepatitis C virus carriers with normal serum aminotransferase based on platelet count. Hepatol Res. 2008;38:27–36.
32. Iwasaki Y, Ikeda H, Araki Y, Osawa T, Kita K, Ando M, et al. Limitation of combination therapy of interferon and ribavirin for older patients with chronic hepatitis. Hepatology. 2006;43:54–63.
33. El-Shamy A, Nagano-Fujii M, Sasase N, Imoto S, Kim SR, Hotta H. Sequence variation in hepatitis C virus nonstructural protein 5A predicts clinical outcome of pegylated interferon/ribavirin combination therapy. Hepatology. 2008;48:38–47.
34. Patton HM, Patel K, Behling C, Bylund D, Blatt LM, Vallee M, et al. The impact of steatosis on disease progression and early and sustained treatment response in chronic hepatitis C patients. J Hepatol. 2004;40:484–90.
35. Lagging M, Romero A, Westin J, Norkrans G, Dhillon AP, Palwlosky JM, et al. IP-10 predicts viral response and therapeutic outcome in difficult-to-treat patients with HCV genotype 1 infection. Hepatology. 2006;44:1617–25.
36. Pilli M, Zerbini A, Penna A, Orlandini A, Lukasiewicz E, Pawlotsky JM, et al. HCV-specific T-cell response in relation to viral kinetics and treatment outcome (DITTO-HCV Project). Gastroenterology. 2007;133:1132–43.
37. Shirakawa H, Matsumoto A, Joshita S, Komatsu M, Tanaka N, Umemura T, et al. Pretreatment prediction of virological response to peginterferon plus ribabirin therapy in chronic hepatitis C patients using viral and host factors. Hepatology. 2008; 48:1753–60.

Integrative Transcriptome Analysis Reveals Common Molecular Subclasses of Human Hepatocellular Carcinoma

Yujin Hoshida,[1,2] Sebastian M.B. Nijman,[1,3] Masahiro Kobayashi,[6] Jennifer A. Chan,[1,7] Jean-Philippe Brunet,[1] Derek Y. Chiang,[1] Augusto Villanueva,[8] Philippa Newell,[10] Kenji Ikeda,[6] Masaji Hashimoto,[6] Goro Watanabe,[6] Stacey Gabriel,[1] Scott L. Friedman,[10] Hiromitsu Kumada,[6] Josep M. Llovet,[8,9,10] and Todd R. Golub[1,2,3,4]

[1]Broad Institute of Massachusetts Institute of Technology and Harvard University, Cambridge, Massachusetts; [2]Pediatric Oncology, Dana-Farber Cancer Institute; [3]Children's Hospital Boston, Harvard Medical School; [4]Howard Hughes Medical Institute, Boston, Massachusetts; [5]Center for Molecular Medicine of the Austrian Academy of Sciences, Vienna, Austria; [6]Toranomon Hospital, Tokyo, Japan; [7]University of Calgary, Calgary, Alberta, Canada; [8]Barcelona-Clinic Liver Cancer Group, Liver Unit, CIBERehd, Hospital Clínic, IDIBAPS; [9]Institució Catalana de Recerca i Estudis Avançats, Barcelona, Spain; and [10]Liver Cancer Program, Mount Sinai School of Medicine, New York, New York

Abstract

Hepatocellular carcinoma (HCC) is a highly heterogeneous disease, and prior attempts to develop genomic-based classification for HCC have yielded highly divergent results, indicating difficulty in identifying unified molecular anatomy. We performed a meta-analysis of gene expression profiles in data sets from eight independent patient cohorts across the world. In addition, aiming to establish the real world applicability of a classification system, we profiled 118 formalin-fixed, paraffin-embedded tissues from an additional patient cohort. A total of 603 patients were analyzed, representing the major etiologies of HCC (hepatitis B and C) collected from Western and Eastern countries. We observed three robust HCC subclasses (termed S1, S2, and S3), each correlated with clinical parameters such as tumor size, extent of cellular differentiation, and serum α-fetoprotein levels. An analysis of the components of the signatures indicated that S1 reflected aberrant activation of the WNT signaling pathway, S2 was characterized by proliferation as well as MYC and AKT activation, and S3 was associated with hepatocyte differentiation. Functional studies indicated that the WNT pathway activation signature characteristic of S1 tumors was not simply the result of *β-catenin* mutation but rather was the result of transforming growth factor-β activation, thus representing a new mechanism of WNT pathway activation in HCC. These experiments establish the first consensus classification framework for HCC based on gene expression profiles and highlight the power of integrating multiple data sets to define a robust molecular taxonomy of the disease. [Cancer Res 2009;69(18):7385–92]

Introduction

Hepatocellular carcinoma (HCC) affects approximately half a million patients worldwide and is the most rapidly increasing cause of cancer death in the United States owing to the lack of effective treatment options for advanced disease (1). Numerous lines of clinical and histopathologic evidence suggest that HCC is a heterogeneous disease, but a coherent molecular explanation for this heterogeneity has yet to be reported. Genomic approaches to the classification of HCC therefore hold promise for a molecular taxonomy of the disease.

Mutations in the WNT signaling pathway have been found to be common in HCC, but other DNA level classification approaches have proven challenging. This relates to the enormous complexity of the genomic alterations observed in HCC, likely attributable to the accumulation of chromosomal rearrangements resulting from decades of chronic viral hepatitis and cirrhosis. This complexity makes it difficult to identify the causal genetic events promoting HCC development and progression (2, 3). An alternate approach to HCC classification has been to study tumors at the level of their gene expression profiles. Although several such profiling efforts have been reported (4–11), a cohesive view of expression-based subclasses of HCC has yet to emerge. In part, this is because each of the reported studies analyzed different patient populations (most of them small) on a different microarray platform, with a different primary biological or clinical question in mind. Perhaps not surprisingly then, each study reported a somewhat different view of the heterogeneity of HCC, and it has been therefore impossible to see whether there exists a common biological thread that links these disparate studies.

We believe that any biologically or clinically meaningful classification system should be informative across multiple patient populations and should be independent of any particular microarray platform. In the present study, we therefore set out to define molecular subclasses of HCC that existed across all available HCC data sets, including eight previously reported studies and one new one reported here, totaling 603 patients. We report that indeed there exist three distinct molecular subclasses of HCC that are present in all nine data sets examined, regardless of technical differences between the microarray platforms used to generate the profiles. We show that these subclasses are correlated with histologic, molecular, and clinical features of HCC, and we highlight the important role of transforming growth factor-β (TGF-β) signaling in one of the HCC subclasses. These findings thus create a solid foundation for HCC classification on which to build informed clinical trials for patients with HCC and also suggest new opportunities for therapeutic intervention.

Note: Supplementary data for this article are available at Cancer Research Online (http://cancerres.aacrjournals.org/).

Requests for reprints: Todd R. Golub, Broad Institute of Massachusetts Institute of Technology and Harvard University, 7 Cambridge Center, Cambridge, MA 02142. Phone: 617-324-0700; Fax: 617-258-0903; E-mail: golub@broad.mit.edu.

doi:10.1158/0008-5472.CAN-09-1089

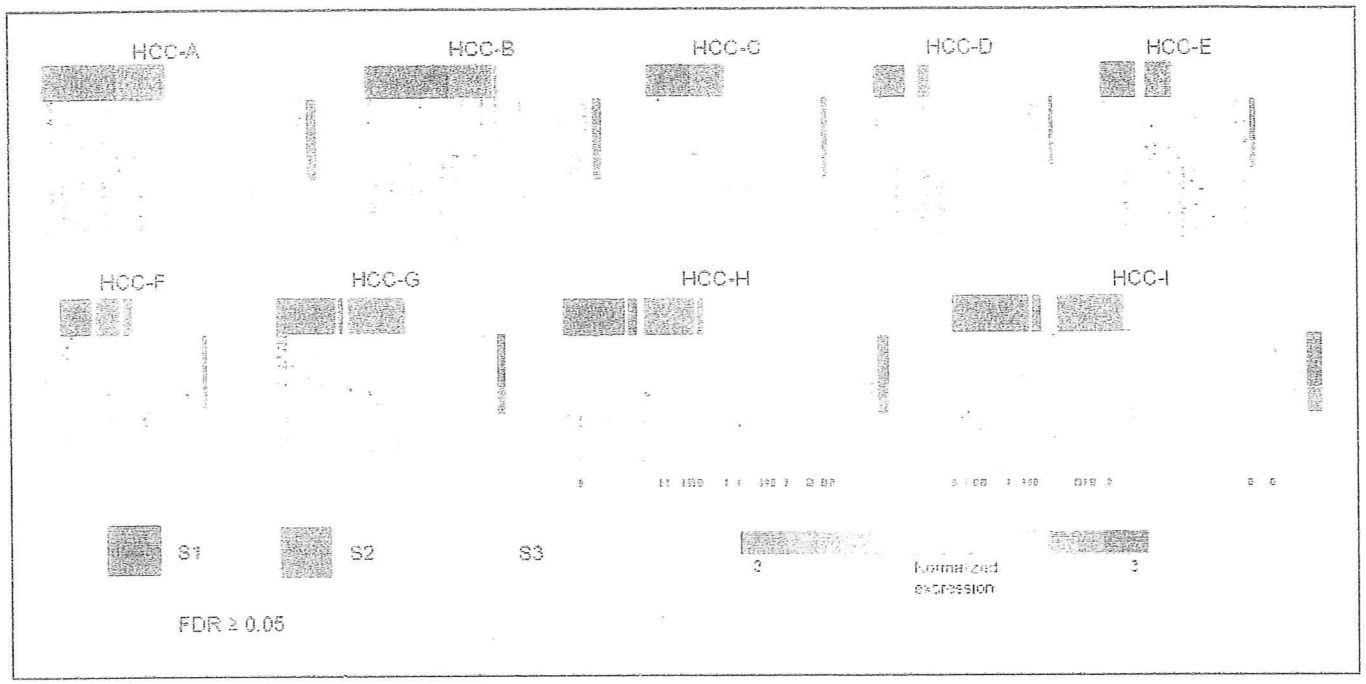

Figure 1. HCC subclasses predicted in nine independent data sets. Predicted subclasses are shown in red (S1), blue (S2), and yellow (S3) with expression pattern of the HCC subclass signature. The proportion of the cases with confident prediction (FDR < 0.05) in HCC-A, HCC-B, HCC-C, HCC-D, HCC-E, HCC-F, HCC-G, HCC-H, and HCC-I were 96%, 96%, 90%, 81%, 79%, 87%, 94%, 83%, and 83%, respectively. Red bars attached to HCC-H and HCC-I indicate positive *β-catenin* mutations and nuclear staining of p53, respectively.

Materials and Methods

Microarray Data Sets and Statistical Analysis

Identification of common HCC subclasses. To define and validate a gene expression–based model of common molecular subclasses of HCC, we collected publicly available gene expression data sets from eight independent cohorts profiled on a wide variety of microarray platforms (HCC-A, HCC-B, HCC-C, HCC-D, HCC-E, HCC-F, HCC-G, and HCC-H; see Supplementary Tables S1 and S2 for details; refs. 4–11). Between the training data sets (HCC-A, HCC-B, and HCC-C) chosen as larger data sets covering major etiologies of HCC to avoid overfitting a model to any particular cohort or microarray platform, corresponding subgroups of the samples were defined by subclass mapping (SubMap) method (12) based on subclasses that identified three unsupervised clustering methods: hierarchical clustering, k-means clustering, and nonnegative matrix factorization, which finds clusters of samples after collapsing the data set into representative "meta-genes" (13).

For each subclass defined by SubMap, meta-analysis marker genes were selected as overexpressed genes compared with the rest of the subclasses (HCC subclass signature) in all the three clustering methods to avoid defining gene expression–based subclasses that were unique to a particular clustering algorithm. Prediction of the subclass was performed for each sample using nearest template prediction method (14, 15) to accommodate the diverse microarray platforms (see Supplementary Data for details).

Molecular annotation of HCC subclasses. Functional characterization of the HCC subclasses was performed using gene set enrichment analysis (GSEA; ref. 16). Two categories of gene sets in Molecular Signature Database (MSigDB)[11] were used: target gene sets regulated by experimental perturbations (377 gene sets) and literature-based manually curated molecular pathway gene sets (130 gene sets).

Clinical data analysis. The hazard of tumor recurrence was calculated to estimate the pattern of HCC recurrence over time after the surgery as previously reported (17, 18). Continuous and proportional data were tested by Wilcoxon rank sum test and Fisher's exact test, respectively. All clinical data analyses were performed using the R statistical package version 2.4.0.[12]

Microarrays for Fixed Tissues

We generated a ninth data set of formalin-fixed, paraffin-embedded (FFPE) tumors (HCC-I), reasoning that any meaningful classification system should be applicable to routinely collected fixed (as opposed to frozen) tissues. We analyzed FFPE tissue blocks from 118 HCC patients who consecutively underwent surgical resection during 1990 to 2001 at Toranomon Hospital. Ethical approval for use of the FFPE tissues, obtained and archived as part of routine clinical care, was acquired from the institutional review board granted on condition that all samples be made anonymous. Total RNA was extracted from macrodissected 10-μm tissue slices (three to four slices for each sample) using High Pure RNA Paraffin kit (Roche). Expression of transcriptionally informative 6,000 genes, selected to capture global state of transcriptome (14), was profiled using DNA-mediated annealing, selection, extension, and ligation (DASL) assay (Illumina; see Supplementary Data; ref. 19).

Microarrays for Cell Lines

Total RNA was isolated using Trizol reagent (Invitrogen) according to the manufacturer's instruction. Microarray experiment was performed using HT_HG-U133A High-Throughput Arrays (Affymetrix). The raw data were normalized using BioConductor affy package.[13]

All microarray data sets are available through National Center for Biotechnology Information Gene Expression Omnibus[14] with accession numbers of GSE10186 (DASL), GSE10393 (U133A), and GPL5474 (transcriptionally informative gene panel for DASL) and our Web site.[15]

[11] http://www.broad.mit.edu/gsea/msigdb/

[12] http://www.r-project.org

[13] http://www.bioconductor.org/

[14] http://www.ncbi.nlm.nih.gov/geo/

[15] http://www.broad.mit.edu/cancer/pub/HCC

Table 1. Clinical phenotypes associated with HCC subclasses

Variable	S1	S2	S3	*P*
Tumor size (cm)*	3.0 [2.0,4.5]	4.5 [2.5,7.0]	2.5 [1.8,4.3]	0.003
Tumor differentiation*				
Well	8 (16%)	4 (10%)	37 (44%)	
Moderate	27 (53%)	23 (59%)	45 (53%)	<0.001
Poor	16 (31%)	12 (31%)	3 (4%)	
AFP (ng/mL)†	50 [14.332]	171 [27.1.251]	13 [5.43]	<0.001
Hepatitis B virus infection‡	39 (38%)	27 (36%)	39 (25%)	0.05
Hepatitis C virus infection‡	55 (53%)	44 (58%)	109 (69%)	0.03

NOTE: Median [25%,75%]. Wilcoxon rank sum test for continuous data, and Fisher's exact test for categorical data.
*HCC-F, HCC-H, and HCC-I: S1, $n = 55$; S2, $n = 46$; S3, $n = 96$.
†HCC-H and HCC-I: S1, $n = 48$; S2, $n = 39$; S3, $n = 83$.
‡HCC-B, HCC-C, HCC-F, HCC-H, and HCC-I: S1, $n = 103$; S2, $n = 76$; S3, $n = 158$.

Immunostaining

Immunohistochemical staining was performed on 10-μm FFPE sections using antibodies for β-catenin (Becton Dickinson), phospho-AKT (Cell Signaling), and p53 (Immunotech) followed by detection using the Envision+ DAB system (Dako). The stains were evaluated by a pathologist blinded to the results of the gene expression profiling, and the results were scored in a binary system. For immunofluorescence staining, cells grown on multiwell chamber slides were fixed by 4% paraformaldehyde and stained for β-catenin (see Supplementary Data for details).

Cell Culture

Human HCC cell lines, Huh-7 (Riken Bioresource Center) and SNU-387 (American Type Culture Collection), were grown in DMEM supplemented with 10% heat-inactivated fetal bovine serum at 37°C in a 5% CO_2 atmosphere. No *β-catenin* mutation has been found in these cell lines.

Western Blotting

Cell lysates were separated on NuPAGE 4% to 12% gels (Invitrogen) and transferred to polyvinylidene difluoride membranes (Bio-Rad) and blotted for α-fetoprotein (AFP; Santa Cruz Biotechnology), β-catenin, phospho-SMAD3 (Cell Signaling), and proliferating cell nuclear antigen (Santa Cruz Biotechnology) antibodies.

β-Catenin Knockdown

Cells were infected with the indicated short hairpin RNA (shRNA) vectors (construct 1, TRCN0000003843; construct 2, TRCN0000003844; The RNAi Consortium[10]) and puromycin selected. Ninety-six hours after infection, cells were counted and seeded in triplicate (20,000/six well). After 10 d, cells were fixed in paraformaldehyde and stained with crystal violet. Dye was extracted with 10% acetic acid and absorbance was determined at 600 nm.

Luciferase Assay

Cells were transfected using Lipofectamine 2000 (Invitrogen) with either TOP-flash or FOP-flash constructs and stimulated with 100 pmol/L TGF-β (R&D Systems) for 48 h. Luciferase activity was measured using Dual-Glo kit (Promega). All transfections were performed in triplicate and measurements were normalized to a SV40 promoter-driven *Renilla* luciferase construct.

Results

Three common molecular subclasses of HCC. The SubMap method identified three robust subclasses in each of the three initial data sets analyzed. We refer to these subclasses as S1, S2, and S3 (Fig. 1), and the complete list of genes that correlated with each of the subclasses is available in Supplementary Table S3. As with any unsupervised clustering–based definition of cancer subclasses, it is essential to establish the validity of the newfound classification system. In the following sections, we describe three independent validations of the three-class structure of HCC. First, we show that the three subclasses are detected with statistical significance in each of the six remaining HCC data sets (totaling 371 patients). Second, we show that the subclasses are associated with clinical parameters. Third, we show that the subclasses are associated with biological mechanism known to be operative in the pathogenesis of HCC.

Statistical validation of subclasses across nine HCC cohorts. As a statistical measure of the validity of the three subclasses, we determined the confidence with which HCC samples could be classified into one of the three subclasses using the HCC subclass signature–based classifier, including 619 genes. As expected, subclass labels were assigned with high confidence [false discovery rate (FDR) < 0.05] to 94% of the training samples (HCC-A, HCC-B, and HCC-C), which were used to define the subclasses in the first place. More importantly, high confidence subclass labels were assigned to 84% of the 371 samples in the validation set (HCC-D, HCC-E, HCC-F, HCC-G, HCC-H, and HCC-I). In contrast, a classifier based on the same number of genes chosen randomly yielded high confidence predictions in <1% of the samples. In addition, our classification system was superior to those reported previously (10, 11, 20, 21) when those classifiers were tested across all of the validation data sets (high confidence predictions using reported signatures were 27–75%; Supplementary Fig. S1). These results, taken together, indicate the statistical significance of our three subclasses and point to the limitation of defining subclasses based on only a single cohort, where overfitting often leads to failure of the classifier to validate on new samples, particularly when profiled on a different microarray platform.

Clinical relevance of HCC subclasses. Having established the statistical validity of the HCC subclasses, we next asked whether any of the subclasses were associated with clinical parameters to add the validity of the subclasses. Clinical data were available for 197 patients, as summarized in Table 1.

Our first observation was that tumors in subclass S2 were larger than the others, whereas tumors in S3 were smaller compared with the rest ($P = 0.003$). In addition, subclass S3 included the majority of well-differentiated tumors (37 of 49; $P < 0.001$), whereas there was no

[10] www.broad.mit.edu/genome_bio/trc/rnai.html

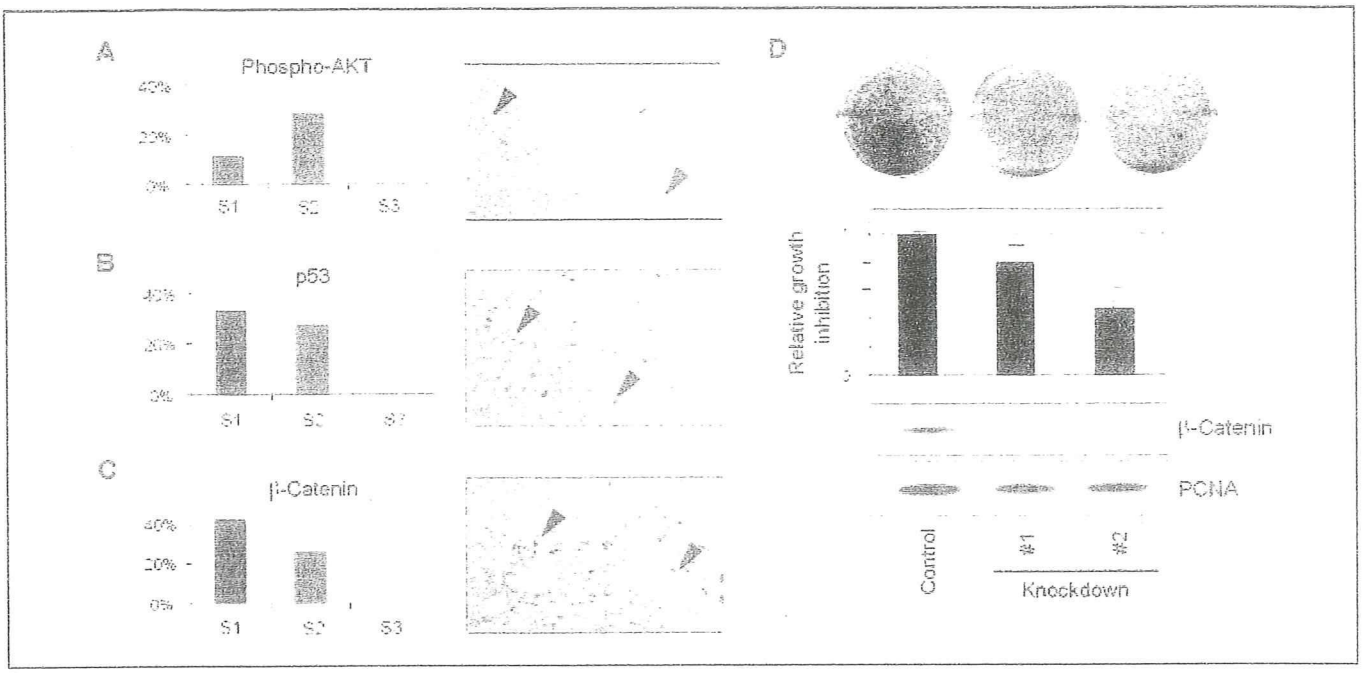

Figure 2. Molecular pathways associated with HCC subclasses. Immunohistochemical analysis of phospho-AKT (*A*), p53 (*B*), and β-catenin (*C*) proteins in HCC-I. *Left*, proportions of the cases with positive staining in each HCC subclass; *right*, representative positive staining (*arrowheads*). Magnification, ×20. *D*, growth inhibition of SNU-387 cells (predicted to be subclass S1) by knocking down β-catenin protein using two different shRNA constructs.

histologic difference between S1 and S2 ($P = 0.73$). We also examined the serum levels of the one clinically used serum biomarker of HCC—AFP. Serum AFP was the highest in S2 (0.001), further supporting the notion that our subclasses are clinically relevant.

Next, we sought to determine whether the HCC subclasses were associated with clinical outcome following surgical resection. We were careful to analyze the two major patterns of HCC recurrence: early recurrence, which is related to residual dissemination of primary tumor cells within the liver, and late recurrence, which is attributable to new primary tumors arising in a hypercarcinogenic state of a cirrhotic liver (17, 18, 22). "Early" recurrence is associated with malignant characteristics of the primary tumor itself, and we reported that it has less effect on patient survival in earlier-stage HCC, in which "late" recurrence is the major determinant of survival (14, 23). We found that subclass S1 was associated with a significantly greater risk of earlier recurrence ($P = 0.03$ within 1 year; Supplementary Fig. S2). This association remained to be significant even after correcting for tumor size in multivariate Cox regression modeling (Supplementary Table S4). Consistent with this observation, S1 tumors exhibited more vascular invasion and satellite lesions (both known risk factors for early recurrence; Supplementary Table S5). These results may suggest that the S1 subclass is associated with a more invasive/disseminative phenotype. Interestingly, we found that a recently reported signature of poor survival defined in patients with more advanced HCC, where early recurrence is the major determinant of survival (4), was associated with S1 and S2, whereas the good survival signature defined in that study was enriched in S3 tumors (Supplementary Table S6), lending further credence to our subclass model. Importantly, our HCC subclasses were not associated with late recurrence, consistent with our recent study indicating that late recurrence is determined not by the characteristics of the tumor itself but rather by the biological state of the surrounding liver at risk (14). Furthermore, consistent with our previous observation, the HCC subclasses showed no association with survival ($P = 0.12$) in our data set (HCC-H) consisting mostly of early-stage tumors.

Molecular pathways associated with HCC subclasses. We next asked whether we could ascribe biological meaning to our validated HCC subclasses. The GSEA results indicated that indeed our HCC subclasses were associated with distinct biological processes, several of which have been implicated in HCC pathogenesis (Supplementary Tables S7 and S8). For example, S2 were tumors associated with a relative suppression of IFN target genes (7), of interest because of the use of IFN as an experimental chemopreventive strategy for HCC. S2 tumors were also enriched in MYC target genes, suggesting that MYC activation is a feature of S2 tumors. Consistent with this observation, we found that a recently reported mouse model of HCC based on MYC overexpression (24) exhibited the S2 subclass signature (Supplementary Fig. S3). S2 tumors were also strongly enriched in a signature of EpCAM positivity (Supplementary Table S6; ref. 25), and in addition, we found that S2 tumors overexpressed *AFP* (consistent with S2 patients having elevated serum AFP levels; Table 1). Lastly, S2 tumors were enriched in a signature of AKT activation (10), and validation experiment indicated a trend toward elevated phosphorylation of AKT as determined by immunohistochemistry ($P = 0.07$; Fig. 2A). An AFP-AKT association has been previously observed (10, 26), and we see here that this association is being driven primarily by S2 tumors. The mechanism of AKT activation in these tumors is not known but likely reflects upstream signaling of the phosphatidylinositol 3-kinase (PI3K) pathway (27). As PI3K inhibitors are now entering clinical development, it may be of value to examine their role in S2 tumors in particular.

GSEA also identified differential activation of p53 and p21 target gene sets, with these genes being more abundantly expressed in S3 tumors compared with S1 and S2, consistent with our observation that S3 tumors tend to be lower grade (Table 1). To further validate this result, we performed

immunohistochemistry for p53, wherein nuclear accumulation of p53 protein is well known to reflect inactivating p53 mutation (28). As predicted by the GSEA analysis, S1 and S2 tumors exhibited significantly greater nuclear p53 staining compared with S3 ($P = 0.001$; Fig. 2*B*). The more well-differentiated nature of S3 tumors was also reflected in the S3 gene expression profile, with S3 tumors exhibiting relatively higher levels of expression of hepatocyte function-related genes involved in glycogen/lipid/alcohol metabolism (*APO/ALDH/ADH* family genes), detoxification (*CYP* family genes), coagulation, and oxygen radical scavenging (*CAT, SOD1*; Supplementary Tables S3, S7, and S8).

WNT pathway activation in S1. The WNT signaling pathway is perhaps the best characterized oncogenic pathway in HCC, with pathway activation occurring through *β-catenin* mutation (specifically via mutation in exon 3 in up to 44% of cases) and less frequently in *AXIN1* (<10% of cases; refs. 2, 3). We addressed WNT status with regard to HCC subclass in two ways. First, we performed GSEA analysis using an experimentally defined WNT activation signature. We found strong enrichment of the WNT signature in subclass S1 compared with S2 or S3 (FDR = 0.03; Supplementary Table S7), suggesting preferential WNT activation in S1 tumors. We validated this result via immunohistochemistry for β-catenin (the principal downstream effector of WNT in HCC) and found that S1 tumors indeed had higher levels of cytoplasmic β-catenin protein expression compared with the other subclasses (0.001), again indicating preferential activation of the canonical WNT pathway in S1 (Fig. 2*C*; ref. 29). In addition, we found that shRNAs targeting *β-catenin* resulted in growth inhibition when introduced into the SNU-387 cell line (predicted to be subclass S1), thereby further supporting the hypothesis that WNT activation is functionally important in S1 tumors (Fig. 2*D*).

Mechanisms of WNT activation in S1 tumors. Having determined that S1 tumors exhibit preferential activation of the WNT/β-catenin pathway, we next addressed potential mechanisms for this activity. We first asked whether the S1 tumors were associated with *β-catenin* mutation in HCC-H data set, for which we previously sequenced exon 3 of *β-catenin* gene (11). Surprisingly, *β-catenin* mutations were preferentially found in S3 tumors, consistent with previously reported "CTNNB1" class representing a subset of S3 (11, 30). This result is also consistent with recent evidence indicating that *β-catenin* mutations do not regulate the canonical WNT target genes (e.g., *cyclin D1* and *MYC*) that characterize our S1-associated WNT activation signature (31). These results further suggest that the WNT pathway is activated in S1 tumors by a mechanism other than *β-catenin* mutation.

To explore alternate explanations for WNT pathway activation, we again turned to GSEA, asking whether other gene sets (signatures) enriched in S1 tumors might provide insight into WNT activation in these tumors. Strikingly, we observed strong overexpression of TGF-β target gene sets (i.e., genes expressed as a result of experimental activation of TGF-β) in S1 tumors (Supplementary Table S7). We similarly observed enrichment of a gene set associated with epithelial-to-mesenchymal transition, a phenomenon implicated in tumor invasion and metastasis (32) and known to be regulated by TGF-β signaling in HCC (Supplementary Table S7; refs. 33, 34). Furthermore, a previously reported TGF-β activation signature associated with an invasive phenotype (35) showed strong enrichment in S1 (Supplementary Table S6). We observed no genomic copy number change associated with S1 subclass in *TGFB1* locus, suggesting that chromosomal aberration is not the causative mechanism of the activation (Supplementary Fig. S4). These results indicate that TGF-β and WNT signaling co-occur in the same HCC subclass (subclass S1), and suggest the hypothesis that TGF-β might in some way lead to WNT activity that defines the S1 molecular phenotype.

TGF-β-WNT interactions. We next explored the hypothesis that TGF-β regulates WNT pathway activity in HCC cells. First, we treated the HCC cell line Huh-7 with intact WNT pathway components (classified as subclass S2 and with no activation of S1 and WNT activation signature) with TGF-β and monitored the genome-wide expression consequence. As predicted, TGF-β stimulation induced expression of WNT target genes (FDR < 0.001; Fig. 3*A*) and induced the expression of genes characteristic of subclass S1 (FDR = 0.04; Fig. 3*B*; Supplementary Data) characterized by WNT/

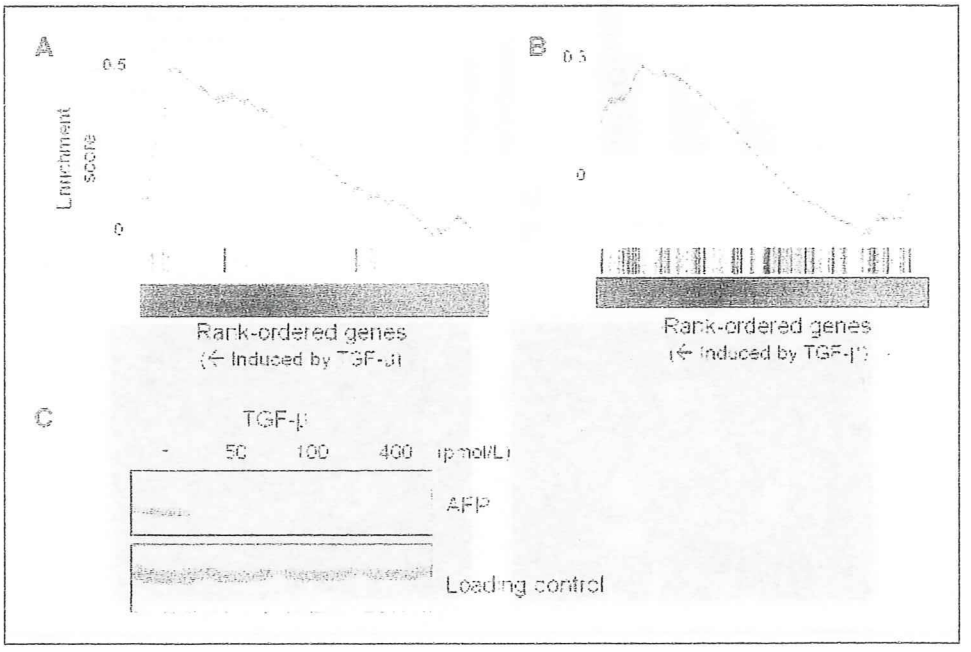

Figure 3. Interaction between WNT pathway and TGF-β. *A*, up-regulation of an experimentally defined WNT target gene set, "KENNY_WNT_UP" (FDR < 0.001), by TGF-β. Genes were rank ordered based on differential expression between TGF-β–treated and untreated Huh-7 cells (predicted to be subclass S2). A database of target gene sets for experimental perturbations (377 gene sets) was assessed by GSEA. *B*, up-regulation of the S1 signature by TGF-β treatment. Genes were rank ordered based on differential expression between treated and untreated Huh-7 cells, and induction of the subclass signature was evaluated by GSEA (FDR = 0.04). *C*, suppression of AFP protein expression by TGF-β treatment. Loading control is nonspecific for AFP antibody to show that equal amounts of protein were loaded.

TGF-β activity while suppressing expression of AFP protein, one of the top markers for S2 (Fig. 3C).

Second, we asked whether TGF-β could regulate the activity of a T-cell factor-lymphoid enhancer factor (TCF-LEF) reporter, further reflecting WNT/β-catenin activity. TGF-β stimulation of Huh-7 cells resulted in activation of a wild-type (TOP-flash) but not mutant (FOP-flash) TCF-LEF luciferase reporter (Fig. 4A). Interestingly, the superactivation of TCF-LEF activity was also observed in the presence of cotransfected mutant β-catenin. These results validate the hypothesis that TGF-β enhances WNT activity in HCC, consistent with the subclass S1 molecular profile.

We next explored the mechanism by which TGF-β augments WNT/β-catenin activity. A simple explanation would be that TGF-β induced expression of β-catenin RNA or protein levels, but we found no evidence for this (Fig. 4B). Strikingly, however, TGF-β treatment resulted in a marked change in β-catenin subcellular localization. Specifically, TGF-β treatment induced a shift from membranous β-catenin staining to a cytoplasmic distribution with focal perinuclear aggregation (Fig. 4C). This suggests that TGF-β enhances WNT signaling by modulating the intracellular pool of free β-catenin.

Taken together, these results validate the observation that TGF-β and WNT activity together typify the S1 subclass of HCC, and further suggest that TGF-β augments WNT activity via alteration of the subcellular localization of β-catenin, consistent with the cross-talk between these pathways observed in other biological contexts (34, 36). This implies that therapeutic cotargeting TGF-β and β-catenin in S1 tumors might be explored as a strategy for the treatment of S1 subclass HCC.

Discussion

Advances in genome technologies are now supporting a breadth of cancer genome characterization studies, including those focusing on HCC. Along with this proliferation of studies has come, however, a certain confusion in the field—different studies often report different results relating to the same set of underlying questions. For example, ~10 articles on the gene expression–based classification of HCC have been published in recent years, but a consensus molecular taxonomy of the disease has yet to emerge. This might lead some to believe that either expression technologies are insufficiently stable or HCC is so hopelessly heterogeneous and complex that regular, reproducible patterns in the data are nonexistent. We report here that in fact a highly reproducible molecular architecture of HCC is identifiable and is detected across all available HCC data sets.

Our analysis of nine HCC data sets totaling 603 patients indicated that there exist three major subclasses of HCC, which we refer to as subclasses S1, S2, and S3 (Fig. 5). Importantly, although the proportion of each subclass varied slightly from study to study, the subclasses were identifiable regardless of the geographic location of the study patients (Asia versus Europe versus United States) or the technology platform used (cDNA versus oligonucleotide arrays, and frozen versus FFPE tissues). Notably, the new data set generated in the present study used FFPE tissues, thereby showing that the three-class structure is readily detectable in specimens collected and stored in the routine clinical setting. This is relevant because the future deployment of diagnostic tests aimed at cancer classification should ideally be applicable to the standard FFPE specimens that are obtained in clinical practice.

Several biological insights can be made from the observed three-class structure of HCC. Class S1 is particularly notable for the prominence of a WNT activation gene expression signature. This is notable because such WNT activation is not simply explained by the presence of activated *β-catenin* mutations, suggesting that additional mechanisms of WNT activation seem to be at play,

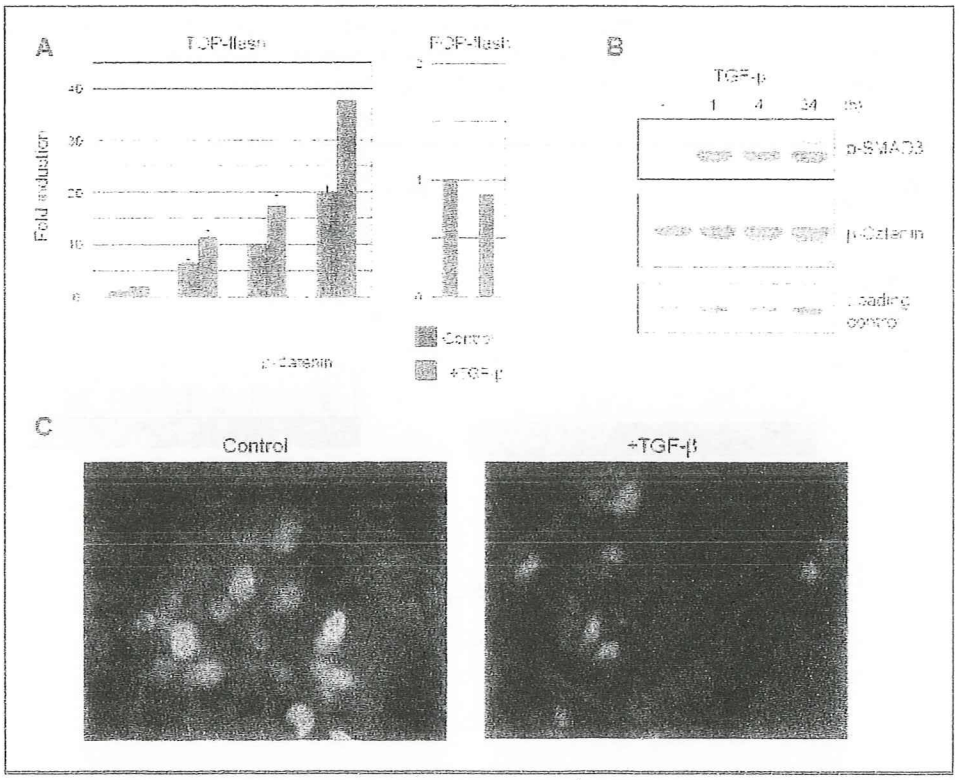

Figure 4. Activation of WNT pathway by TGF-β. *A*, Huh-7 cells were transfected with the indicated reporter constructs and increasing amounts of mutant β-catenin (2, 5, and 10 ng of plasmid). *B*, TGF-β pathway activation was confirmed by phosphorylation of SMAD3. Abundance of β-catenin protein was not changed by TGF-β treatment (100 pmol/L, 48 h). Loading control is nonspecific for phospho-SMAD3 antibody to show that equal amounts of protein were loaded. *C*, Huh-7 cells were stimulated as above and stained for β-catenin. Cellular distribution of β-catenin changed from predominantly membranous to cytoplasmic and perinuclear, and clustered cells spread out with more elongated and flattened morphology.

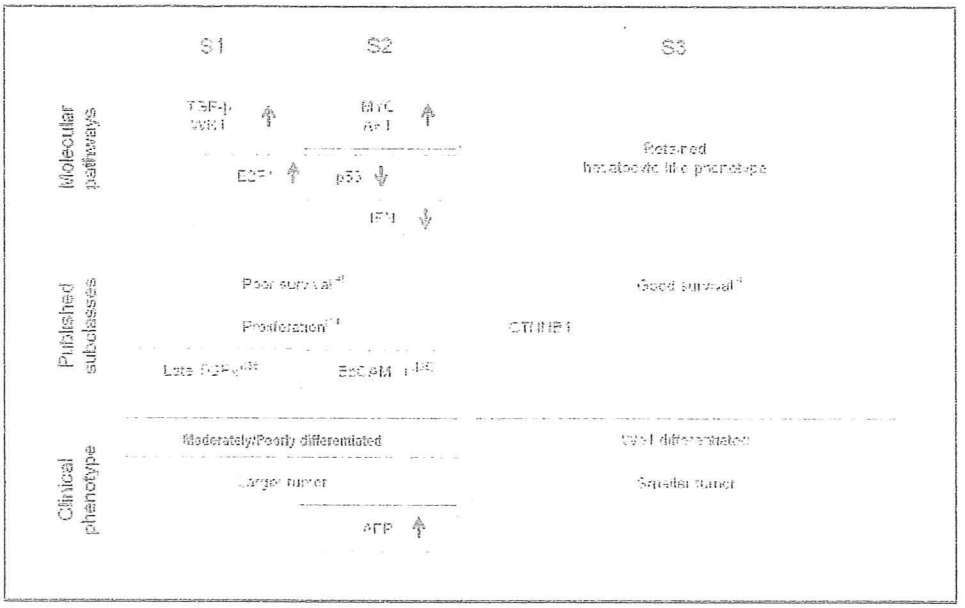

Figure 5. Schematic summary of the characteristics of HCC subclasses.

including TGF-β activation. This may be particularly important in the setting of clinical trials testing β-catenin inhibitors in HCC. Our data suggest that such inhibitors may be worth exploring in HCC beyond those patients harboring *β-catenin* mutation. Although additional mechanistic studies are clearly required, our data support the existence of an interaction between WNT activation and TGF-β activation in S1 tumors, an interaction that has been recently proposed in HCC (34).

Class S2 tumors were notable for their high level of expression of *AFP*, associated with elevated plasma levels of AFP protein compared with non-S2 patients. S2 tumors also tended to be enriched in MYC tumors harboring a MYC activation signature. This is of relevance because it suggests that genetically engineered mouse models of HCC based on MYC activation may be used to interrogate biological basis of the S2 subclass of human HCC. In addition, the finding of an AKT activation signature in S2 tumors suggests that AKT or PI3K inhibitors might be particularly worthy of exploration in this subclass. Further studies are required to establish the mechanism by which AKT is activated in these tumors.

S3 tumors were notable for their relative histologic evidence of differentiation, and the S3 gene expression program was accordingly suggestive of a molecular program of differentiated hepatocyte function. It is tempting to speculate that these tumors might be particularly well suited to differentiation therapy with agents such as retinoids, as has been previously suggested (37). Whether S3 tumors have distinct mechanisms of transformation or rather simply allow for more complete cellular differentiation remains to be determined. The preserved p53 function in S3 suggests that the abrogation of p53 is associated with stepwise malignant transformation of well-differentiated tumors rather than initiation of carcinogenesis. The less frequent *β-catenin* mutations in S1 and S2 may suggest that these tumors arose through different carcinogenic mechanisms compared with S3.

Clearly, much remains to be learned about the biological basis of our observed HCC subclasses. But the fact that they are observed in all studies of HCC examined to date suggests that they represent a reproducible classification framework for the disease. We therefore propose that it will be important to know the subclass of HCC patients entering clinical trials for the treatment of HCC because the response to targeted agents (e.g., β-catenin and PI3K) is likely to be different across the subsets (38). Early observations of differential sensitivity of these distinct tumor types may help guide the design of future clinical trials aimed at targeting agents to distinct patient populations.

Disclosure of Potential Conflicts of Interest

No potential conflicts of interest were disclosed.

Acknowledgments

Received 3/25/09; revised 6/9/09; accepted 6/18/09; published OnlineFirst 9/1/09.

Grant support: NIH/National Cancer Institute grant 5U54 CA112962-03 (T.R. Golub), NIH/National Institutes of Diabetes, Digestive and Kidney Diseases grant 1R01DK076986 (J.M. Llovet), NIH (Spain) grant I+D Program SAF-2007-61898 (J.M. Llovet), and Samuel Waxman Cancer Research Foundation. Y. Hoshida is supported by Charles A. King Trust fellowship. S.M.B. Nijman was supported by the Netherlands Organisation for Scientific Research (Rubicon) and Dutch Cancer Society fellowships.

The costs of publication of this article were defrayed in part by the payment of page charges. This article must therefore be hereby marked *advertisement* in accordance with 18 U.S.C. Section 1734 solely to indicate this fact.

We thank Menno Creyghton for reagents and helpful suggestion; So Young Kim, Ron Firestein, William Hahn, and David Root for the shRNA constructs; Megan Hanna for technical help; Weijia Zhang for critical reading of the manuscript; and Jadwiga Grabarek and Mariko Kobayashi for general support.

References

1. El-Serag HB, Rudolph KL. Hepatocellular carcinoma: epidemiology and molecular carcinogenesis. Gastroenterology 2007;132:2557–76.
2. Farazi PA, DePinho RA. Hepatocellular carcinoma pathogenesis: from genes to environment. Nat Rev Cancer 2006;6:674–87.
3. Villanueva A, Newell P, Chiang DY, Friedman SL, Llovet JM. Genomics and signaling pathways in hepatocellular carcinoma. Semin Liver Dis 2007;27:55–76.
4. Lee JS, Chu IS, Heo J, et al. Classification and prediction of survival in hepatocellular carcinoma by gene expression profiling. Hepatology 2004;40:667–76.
5. Chen X, Cheung ST, So S, et al. Gene expression patterns in human liver cancers. Mol Biol Cell 2002;13:1929–39.
6. Iizuka N, Oka M, Yamada-Okabe H, et al. Oligonucleotide

microarray for prediction of early intrahepatic recurrence of hepatocellular carcinoma after curative resection. Lancet 2003;361:923–9.
7. Breuhahn K, Vreden S, Haddad R, et al. Molecular profiling of human hepatocellular carcinoma defines mutually exclusive interferon regulation and insulin-like growth factor II overexpression. Cancer Res 2004;64:6058–64.
8. Ye QH, Qin LX, Forgues M, et al. Predicting hepatitis B virus-positive metastatic hepatocellular carcinomas using gene expression profiling and supervised machine learning. Nat Med 2003;9:416–23.
9. Midorikawa Y, Tsutsumi S, Nishimura K, et al. Distinct chromosomal bias of gene expression signatures in the progression of hepatocellular carcinoma. Cancer Res 2004;64:7263–70.
10. Boyault S, Rickman DS, de Reynies A, et al. Transcriptome classification of HCC is related to gene alterations and to new therapeutic targets. Hepatology 2007;45:42–52.
11. Chiang DY, Villanueva A, Hoshida Y, et al. Focal gains of VEGFA and molecular classification of hepatocellular carcinoma. Cancer Res 2008;68:6779–88.
12. Hoshida Y, Brunet JP, Tamayo P, Golub TR, Mesirov JP. Subclass mapping: identifying common subtypes in independent disease data sets. PLoS ONE 2007;2:e1195.
13. Brunet JP, Tamayo P, Golub TR, Mesirov JP. Metagenes and molecular pattern discovery using matrix factorization. Proc Natl Acad Sci U S A 2004;101:4164–9.
14. Hoshida Y, Villanueva A, Kobayashi M, et al. Gene expression in fixed tissues and outcome in hepatocellular carcinoma. N Engl J Med 2008;359:1995–2004.
15. Xu L, Shen SS, Hoshida Y, et al. Gene expression changes in an animal melanoma model correlate with aggressiveness of human melanoma metastases. Mol Cancer Res 2008;6:760–9.
16. Subramanian A, Tamayo P, Mootha VK, et al. Gene set enrichment analysis: a knowledge-based approach for interpreting genome-wide expression profiles. Proc Natl Acad Sci U S A 2005;102:15545–50.
17. Imamura H, Matsuyama Y, Tanaka E, et al. Risk factors contributing to early and late phase intrahepatic recurrence of hepatocellular carcinoma after hepatectomy. J Hepatol 2003;38:200–7.
18. Mazzaferro V, Romito R, Schiavo M, et al. Prevention of hepatocellular carcinoma recurrence with α-interferon after liver resection in HCV cirrhosis. Hepatology 2006;44:1543–54.
19. Fan JB, Yeakley JM, Bibikova M, et al. A versatile assay for high-throughput gene expression profiling on universal array matrices. Genome Res 2004;14:878–85.
20. Kaposi-Novak P, Lee JS, Gomez-Quiroz L, Coulouarn C, Factor VM, Thorgeirsson SS. Met-regulated expression signature defines a subset of human hepatocellular carcinomas with poor prognosis and aggressive phenotype. J Clin Invest 2006;116:1582–95.
21. Lee JS, Heo J, Libbrecht L, et al. A novel prognostic subtype of human hepatocellular carcinoma derived from hepatic progenitor cells. Nat Med 2006;12:410–6.
22. Bruix J, Sherman M. Management of hepatocellular carcinoma. Hepatology 2005;42:1208–36.
23. Hoshida Y, Villanueva A, Llovet JM. Molecular profiling to predict hepatocellular carcinoma outcome. Expert Rev Gastroenterol Hepatol 2009;3:101–3.
24. Lee JS, Chu IS, Mikaelyan A, et al. Application of comparative functional genomics to identify best-fit mouse models to study human cancer. Nat Genet 2004;36:1306–11.
25. Yamashita T, Forgues M, Wang W, et al. EpCAM and α-fetoprotein expression defines novel prognostic subtypes of hepatocellular carcinoma. Cancer Res 2008;68:1451–61.
26. Sahin F, Kannangai R, Adegbola O, Wang J, Su G, Torbenson M. mTOR and P70 S6 kinase expression in primary liver neoplasms. Clin Cancer Res 2004;10:8421–5.
27. Villanueva A, Chiang DY, Newell P, et al. Pivotal role of mTOR signaling in hepatocellular carcinoma. Gastroenterology 2008;135:1972–83.
28. Vousden KH, Lane DP. p53 in health and disease. Nat Rev Mol Cell Biol 2007;8:275–83.
29. Miller JR, Moon RT. Signal transduction through β-catenin and specification of cell fate during embryogenesis. Genes Dev 1996;10:2527–39.
30. Thorgeirsson SS, Lee JS, Grisham JW. Functional genomics of hepatocellular carcinoma. Hepatology 2006;43:S145–50.
31. Zucman-Rossi J, Benhamouche S, Godard C, et al. Differential effects of inactivated Axin1 and activated β-catenin mutations in human hepatocellular carcinomas. Oncogene 2007;26:774–80.
32. Zavadil J, Bottinger EP. TGF-β and epithelial-to-mesenchymal transitions. Oncogene 2005;24:5764–74.
33. Giannelli G, Bergamini C, Fransvea E, Sgarra C, Antonaci S. Laminin-5 with transforming growth factor-β1 induces epithelial to mesenchymal transition in hepatocellular carcinoma. Gastroenterology 2005;129:1375–83.
34. Fischer AN, Fuchs E, Mikula M, Huber H, Beug H, Mikulits W. PDGF essentially links TGF-β signaling to nuclear β-catenin accumulation in hepatocellular carcinoma progression. Oncogene 2007;26:3395–405.
35. Coulouarn C, Factor VM, Thorgeirsson SS. Transforming growth factor-β gene expression signature in mouse hepatocytes predicts clinical outcome in human cancer. Hepatology 2008;47:2059–67.
36. Jian H, Shen X, Liu I, Semenov M, He X, Wang XF. Smad3-dependent nuclear translocation of β-catenin is required for TGF-β1-induced proliferation of bone marrow-derived adult human mesenchymal stem cells. Genes Dev 2006;20:666–74.
37. Muto Y, Moriwaki H, Ninomiya M, et al. Prevention of second primary tumors by an acyclic retinoid, polyprenoic acid, in patients with hepatocellular carcinoma. Hepatoma Prevention Study Group. N Engl J Med 1996;334:1561–7.
38. Llovet JM, Bruix J. Molecular targeted therapies in hepatocellular carcinoma. Hepatology 2008;48:1312–27.

Hepatol Int (2009) 3:403–410
DOI 10.1007/s12072-008-9108-8

CASE REPORT

Two cases of development of entecavir resistance during entecavir treatment for nucleoside-naive chronic hepatitis B

Haruhiko Kobashi · Shin-ichi Fujioka · Mitsuhiko Kawaguchi · Hiromitsu Kumada · Osamu Yokosuka · Norio Hayashi · Kazuyuki Suzuki · Takeshi Okanoue · Michio Sata · Hirohito Tsubouchi · Chifumi Sato · Kendo Kiyosawa · Kyuichi Tanikawa · Taku Seriu · Hiroki Ishikawa · Akinobu Takaki · Yoshiaki Iwasaki · Toshiya Osawa · Toshiyuki Takaki · Kosaku Sakaguchi · Yasushi Shiratori · Kazuhide Yamamoto · Daniel J. Tenney · Masao Omata

Received: 27 June 2008 / Accepted: 2 October 2008 / Published online: 9 December 2008

Abstract
Background Entecavir (ETV) is a potent nucleoside analogue against hepatitis B virus (HBV), and emergence of drug resistance is rare in nucleoside-naive patients because development of ETV resistance (ETVr) requires at least three amino acid substitutions in HBV reverse transcriptase. We observed two cases of genotypic ETVr with viral rebound and biochemical breakthrough during

H. Kobashi (✉) · A. Takaki · Y. Iwasaki · K. Sakaguchi · Y. Shiratori · K. Yamamoto
Department of Gastroenterology and Hepatology, Graduate School of Medicine, Dentistry, and Pharmaceutical Sciences, Okayama University, Okayama, Japan
e-mail: hkobashi@md.okayama-u.ac.jp

S.-i. Fujioka · M. Kawaguchi · T. Osawa · T. Takaki
Department of Medicine, Okayama Saiseikai General Hospital, Okayama, Japan

H. Kumada
Center of Liver Disease, Toranomon Hospital, Kanagawa, Japan

O. Yokosuka
Department of Medicine and Clinical Oncology, Graduate School of Medicine, Chiba University, Chiba, Japan

N. Hayashi
Department of Gastroenterology and Hepatology, Graduate School of Medicine, Osaka University, Osaka, Japan

K. Suzuki
First Department of Internal Medicine, Iwate Medical University, Morioka, Japan

T. Okanoue
Molecular Gastroenterology and Hepatology, Graduate School of Medical Science, Kyoto Prefectural University of Medicine, Kyoto, Japan

M. Sata
Department of Gastroenterology, Kurume University School of Medicine, Fukuoka, Japan

H. Tsubouchi
Digestive Disease and Life-style Related Disease Health Research, Human and Environmental Sciences, Graduate School of Medical and Dental Sciences, Kagoshima University, Kagoshima, Japan

C. Sato
Department of Analytical Health Science, Graduate School of Allied Health Sciences, Tokyo Medical and Dental University, Tokyo, Japan

K. Kiyosawa
Division of Hepatology and Gastroenterology, Department of Internal Medicine, Shinshu University School of Medicine, Matsumoto, Japan

K. Tanikawa
International Institute for Liver Research, Kurume University, Kurume, Japan

T. Seriu · H. Ishikawa
Bristol-Myers Squibb Japan, Pharmaceutical Research Institute, Tokyo, Japan

D. J. Tenney
Bristol-Myers Squibb, Research and Development, Wallingford, CT, USA

M. Omata
Department of Gastroenterology, Faculty of Medicine, University of Tokyo, Tokyo, Japan

ETV treatment of nucleoside-naive patients with chronic hepatitis B (CHB).

Results *Case 1*: A 44-year-old HBeAg-positive man received ETV 0.1 mg/day for 52 weeks and 0.5 mg/day for 96 weeks consecutively. HBV DNA was 10.0 $\log_{10}$ copies/ml at baseline, declined to a nadir of 3.1 at week 100, and rebounded to 4.5 at week 124 and 6.7 at week 148. Alanine aminotransferase (ALT) level increased to 112 IU/l at week 148. Switching to a lamivudine (LVD)/adefovir-dipivoxil combination was effective in decreasing HBV DNA. *Case 2*: A 47-year-old HBeAg-positive man received ETV 0.5 mg/day for 188 weeks. HBV DNA was 8.2 $\log_{10}$ copies/ml at baseline, declined to a nadir of 2.9 at week 124, and then rebounded to 4.7 at week 148 and 6.4 at week 160. ALT level increased to 72 IU/l at week 172. The ETVr-related substitution (S202G), along with LVD-resistance-related substitutions (L180M and M204V), was detected by sequence analysis at week 124 in both case 1 and case 2.

Conclusions ETVr emerged in two Japanese nucleoside-naive CHB patients after prolonged therapy and incomplete suppression and in one patient after <0.5 mg of dosing. ETV patients with detectable HBV DNA or breakthrough after extended therapy should be evaluated for compliance to therapy and potential emergence of resistance.

Keywords Entecavir · HBV · Chronic hepatitis B · Drug resistance · Nucleoside-naive

Introduction

Hepatitis B virus (HBV) infection is a serious health problem because of its high prevalence, estimated to be infecting more than 350 million people worldwide, and its potential for inducing chronic hepatitis, cirrhosis, hepatic decompensation, and hepatocellular carcinoma (HCC) [1, 2]. It has been demonstrated that the most potent risk factor for development of cirrhosis or HCC is serum HBV DNA level [3, 4], and it seems that suppressing serum HBV load is essential for improving the prognosis of HBV carriers. Treatment of chronic hepatitis B (CHB) has evolved markedly with the introduction of nucleoside-analogue antivirals, that is, lamivudine (LVD), adefovir-dipivoxil (ADV), entecavir (ETV), and telbivudine, to clinical practice. LVD, the first approved nucleoside analogue against HBV, was shown to be effective in suppressing HBV DNA replication, improving transaminase levels, improving liver histology, inducing hepatitis B e antigen (HBeAg) seroconversion, and suppressing hepatic insufficiency and hepatocarcinogenesis in CHB and compensated cirrhosis [5, 6]. However, the effectiveness of LVD is limited because of frequent development of drug resistance followed by a hepatitis flare and, occasionally, hepatic failure [7, 8].

ETV, a novel anti-HBV nucleoside analogue, has more than 1,500 times greater potency than LVD in vitro [9]. In clinical trials, ETV administration demonstrated potent anti-HBV activity with a marked decline in serum HBV DNA level and a significant improvement in liver histology than LVD in nucleoside-naive HBeAg-positive and -negative patients [10, 11]. In addition, emergence of ETV resistance (ETVr) or viral rebound was shown in these studies to be rare. From these results, recent treatment guidelines have recommended ETV as the first-line nucleoside analogue for nucleoside-naive CHB patients, including those with cirrhosis [12, 13].

It has been reported that the development of ETVr in nucleoside-naive patients is very rare, even after 4 years of therapy. Recently, however, rare cases of ETVr, which developed in nucleoside-naive patients in clinical studies, have been reported [14–16]. We also observed two patients who developed ETVr-associated HBV reverse transcriptase (RT) substitutions, followed by *virologic rebound*, defined as an elevation in serum HBV DNA of more than 1 $\log_{10}$ copy/ml from nadir, and biochemical breakthrough in long-term ETV treatment of nucleoside-naive CHB patients. In this article, we report these two cases in detail.

Case report

Case 1

A 44-year-old Japanese male CHB patient was positive for hepatitis B surface antigen (HBsAg), HBeAg, serum HBV DNA, and had HBV genotype C, had elevated alanine aminotransferase (ALT) levels, and had no history of nucleoside analogue treatment. The patient had a history of acute appendicitis at age 30, ureteral stone at age 35, and hyperlipidemia at age 43. He had a habit of drinking alcohol (700 ml) daily but did not smoke. At age 27, he was diagnosed for the first time by health screening as an asymptomatic HBV carrier in the immune-tolerant phase, defined by HBsAg positivity and normal liver enzymes, and he was followed up regularly elsewhere with blood tests for liver enzymes. He was found to have ALT elevation. He was referred to our hospital at age 44 and was diagnosed with CHB. Serum HBV DNA level determined by Roche Amplicor™ Monitor PCR assay (lower limit of detection is 2.6 $\log_{10}$ copies/ml = 400 copies/ml; Roche Diagnostics K.K., Tokyo, Japan) [17] was 10.0 $\log_{10}$ copies/ml and serum ALT level was 199 IU/l. Histologic diagnosis by percutaneous liver biopsy at baseline revealed chronic hepatitis with mild fibrosis and mild activity (CH F1/A1, according to the New Inuyama Classification) [18].

Table 1 Baseline characteristics

	Normal range	Unit	Case 1	Case 2
Age	–	–	44 years	47 years
Gender	–	–	Male	Male
T. Bil	0.2–1.0	mg/dl	0.8	0.5
AST	10–40	IU/l	113	48
ALT	5–40	IU/l	199	74
ALP	115–359	IU/l	268	216
BUN	6–20	mg/dl	9.5	15.9
CREA	0.61–1.04	mg/dl	0.95	0.83
ALB	4.0–5.0	g/dl	4.2	4.3
WBC	3500–8500	/μl	6,800	5,650
Hb	13.5–17.0	g/dl	15.7	14.8
PLT	13.1–36.2	10^4/μl	18.9	14.5
Prothrombin time	10–13	second	10.8	11.2
INR		–	1.0	0.9
HBsAg (CLIA)	0–0.05	IU/ml	>100 (positive)	>100 (positive)
anti-HBs (CLIA)	0–10	IU/ml	0 (negative)	0 (negative)
HBeAg (CLIA)	0–1		120 (positive)	190 (positive)
anti-HBe (CLIA)	0–50	%	<35 (negative)	0 (negative)
HBV DNA (PCR)	<2.6	$\log_{10}$ copies/ml	10.0	8.2
HBV genotype			Genotype C	Genotype C
YMDD (sequencing)			YMDD+	YMDD+
			YVDD–	YVDD–
			YIDD–	YIDD–
Liver histology[a]			CH F1/A1	CH F2/A2

[a] Diagnosed according to New Inuyama classification. T. Bil: total bilirubin, AST: aspartate aminotransferase, ALT: alanine aminotransferase, ALP: alkalinephosphatase, BUN: blood urea nitrogen, CREA: serum creatinine, ALB: serum albumin, WBC: white blood cell count, Hb: hemoglobin, PLT: platelet count, INR: international normalized ratio, HBsAg: hepatitis B surface antigen, CLIA: chemiluminescent immunoassay, anti-HBs: antibody to hepatitis B surface antigen, HBeAg: hepatitis B e antigen, anti-HBe: antibody to hepatitis B e antigen, HBV: hepatitis B virus, PCR: polymerase chain reaction, YMDD: tyrosine-methionine-aspartate-aspartate motif, YVDD: tyrosine-valine-aspartate-aspartate motif, YIDD: tyrosine-isoleucine-aspartate-aspartate motif, CH F1/A1: chronic hepatitis with mild fibrosis and mild activity, CH F2/A2: chronic hepatitis with moderate fibrosis and moderate activity

Other baseline characteristics are shown in Table 1. He was enrolled in a phase II clinical trial of ETV and was randomized into 0.1- and 0.5-mg dosage groups. The trial was conducted in Japan in compliance with the ethical principles of the Declaration of Helsinki, Good Clinical Practice guidelines, and Articles/Notifications of the Ministry of Health, Labor and Welfare (H. Kobashi et al., J Gastroenterol Hepatol, in press). He was assigned into the 0.1-mg dosage group and administered ETV at daily dose of 0.1 mg for an initial 52 weeks. Subsequently, he was administered ETV continuously at a daily dose of 0.5 mg for the following 96 weeks. The serum HBV DNA level, which was 10.0 $\log_{10}$ copies/ml at baseline, declined to a nadir of 3.1 $\log_{10}$ copies/ml at week 88 of ETV treatment. Thereafter, HBV DNA level increased from 4.5 $\log_{10}$ copies/ml at week 124 to 6.3 $\log_{10}$ copies/ml at week 140 and 6.7 $\log_{10}$ copies/ml at week 148. ALT levels increased from 28 IU/l at week 144 to 112 IU/l at week 148. The patient discontinued ETV therapy at week 148, and then received a combination therapy of 100 mg of LVD and 10 mg of ADV per day. Afterwards, HBV DNA level dropped to below 2.6 $\log_{10}$ copies/ml and ALT level was normalized after 28 weeks of LVD/ADV dosing (Fig. 1).

HBV DNA sequence analysis was performed using PCR-amplified HBV DNA from preserved serum samples at baseline and at every 24 weeks via HBV DNA polymerase sequence assay (developed at SRL, Inc., Tokyo, Japan). Although sequence analysis of the baseline isolate revealed no substitution in the RT domain of the HBV DNA polymerase gene, analysis of the isolates collected over time revealed the M204I substitution at week 100 and the L180M, S202G, and M204V substitutions at weeks 124 and 144, respectively (Table 2). In addition, a polymorphic residue N238 was found as mixed N238 N/H at week 100 and thereafter. The